

Metabolic flux analysis for calcium dependent antibiotic (CDA) production in *Streptomyces coelicolor*

Hong Bum Kim,^a Colin P. Smith,^b Jason Micklefield,^c and Ferda Mavituna^{a,*}

^a Chemical Engineering Department, UMIST, Sackville Street, PO Box 88, Manchester M60 1QD, UK

^b Department of Biomolecular Sciences, UMIST, Sackville Street, PO Box 88, Manchester M60 1QD, UK

^c Department of Chemistry, UMIST, Sackville Street, PO Box 88, Manchester M60 1QD, UK

Received 10 September 2003; received in revised form 8 April 2004; accepted 26 April 2004

Available online 9 June 2004

Abstract

The calcium dependent antibiotic (CDA) is a nonribosomal lipopeptide produced by *Streptomyces coelicolor*. We constructed a metabolic network of more than 400 reactions for the primary and secondary metabolism of *S. coelicolor* and used computational metabolic flux balancing to investigate some of the factors affecting growth and production of CDA. Computational results indicated that the CDA production was concomitant with growth. Computational specific growth rates were twice as high as the experimental specific growth rates. Metabolic flux distributions and sensitivity analyses computed for various phases of the batch culture indicated that the specific CDA production rate was affected by nitrogen assimilation, pentose phosphate pathway, shikimate biosynthesis, and oxoglutarate fluxes. Consequently, these metabolic targets were tested using genetic deletions in the model which increased the in silico specific CDA production rate.

© 2004 Elsevier Inc. All rights reserved.

Keywords: Metabolic flux analysis; CDA; *Streptomyces coelicolor*; Nonribosomal peptide synthetases; In silico; Mutasynthesis

1. Introduction

The calcium dependent antibiotic (CDA) of *Streptomyces coelicolor* belongs to a class of natural products called nonribosomal polypeptides. The biosynthesis of these compounds is directed by nonribosomal peptide synthetases which are large multifunctional enzymes. Nonribosomal peptides contain proteinogenic as well as many unusual amino acids. CDA consists of an *N*-terminal *trans*-2,3-epoxyhexanoyl fatty acid side chain and several nonproteinogenic amino acid residues (Kempter et al., 1997). CDA kills other gram-positive bacteria only in the presence of calcium ions; for this reason it was called “calcium dependent” (Hopwood and Wright, 1983). Although the mode of action of the CDA is not known, it is probably similar to the other structurally related acidic lipopeptide antibiotics such as

daptomycin, friulimicins and amphomycins. The antibiotic activity of daptomycin is postulated to be due to disruption of multiple aspects of membrane function. This distinct and potent mechanism of action makes the daptomycin-related compounds, including CDA, important weapons against severe antibiotic resistant pathogens, such as methicillin-resistant *S. aureus* strains (MRSA) and vancomycin-resistant enterococci (VRE). Indeed recently, daptomycin successfully completed phase III clinical trials and became the first acidic lipopeptide antibiotic of its class to be approved for clinical use under the tradename Cubicin (Raja et al., 2003).

The 82 kb region of the *S. coelicolor* genome that encodes the biosynthetic enzymes required for the production of the CDA was sequenced in its entirety as part of the *S. coelicolor* genome project (Chong et al., 1998; Bentley et al., 2002). Some functions have also been suggested for these genes (Ryding et al., 2002) and the sequence of the CDA gene cluster was used recently to determine a putative pathway for the CDA biosynthesis (Hojati et al., 2002).

*Corresponding author. Tel.: +44-161-200-4372/4340; fax: +44-161-200-4399.

E-mail address: f.mavituna@umist.ac.uk (F. Mavituna).

Nomenclature			
AcCoA	acetyl-CoA	ICit	isocitrate
AdoHcy	S-adenosyl-homocysteine	MaCoA	malonyl CoA
AdoMet	S-adenosyl-methionine	Mal	malate
ADP	adenosine 5-diphosphate	MeGlu	3-methyl-glutamic acid
AMP	adenosine 5-phosphate	MeTHF	5 and 10-methylene-THF
Asn	L-asparagine	MOG	beta-methyl-alfa-ketoglutarate
Asp	L-aspartate	NAD	nicotineamide-adeninedinucleotide
ATP	adenosine 5-triphosphate	NADH	nicotineamide-adeninedinucleotide, reduced
CbmP	carbamoyl-phosphate	NADP	nicotineamide-adeninedinucleotide phosphate
CDA4a	CDA4a	NADPH	nicotineamide-adeninedinucleotide phosphate
CDA4b	CDA4b	NH ₂	hydroxylamine
CDAx	CDA compound including L-asparagine	NH ₃	ammonia
Cit	citrate	NO	nitroxyl
CO ₂	carbondioxide	O ₂	oxygen
CoA	coenzyme A	OA	oxaloacetate
CoAthio	coenzyme A-thioester	OG	2-oxoglutarate or alfa-ketoglutarate
Cys	L-cysteine	PEP	4-hydroxy-phenyl pyruvate
Cyst	L-cystathionine	PGA3	D-glyceraldehyde-3-phosphate
E4P	D-erythrose 4-phosphate	PGnL6	6-phosphoglucono-1 and 5-lactone
EpHCoA	trans-epoxyhexanoyl CoA	Pi	inorganic orthophosphate
F6P	beta-D-fructose 6-phosphate	PLP	pyridoxal 5-phosphate
FAD	flavine adenine dinucleotide	PMP	pyrodoxamine 5-phosphate
FADH ₂	flavine adenine dinucleotide reduced	PPi	inorganic pyrophosphate
FADH-OH	flavin-C4a-hydroxide	Prep	prephenate
FADH-OOH	flavin-C4a-hydroperoxide	PShik3	shikimate 3-phosphate or 5-phospho shikimate
Form	formate	Pyr	pyruvate
Form10THF	10-formyl-tetrahydrofolate	S7P	D-sedoheptulose 7-phosphate
G6P	alfa-D-glucose 6-phosphate	Ser	L-serine
GL3P	sn-glycerol 3-phosphate	Shik	shikimate
Gln	L-glutamine	Suc	succinate
Glu	L-glutamate	SucCoA	succinyl-CoA
Glx	glyoxylate	SucHse	O-succinyl-L-homoserine
Gly	glycine	TehCoA	trans-epoxyhexanoyl CoA
Gro	glycerol	ThexCoA	trans-hexenoyl CoA
Hexaa	hexanoic acid	THF	6 (S) -5, 6, 7, and 8-tetrahydrofolate
Hmana	4-hydroxy mandelic acid	Thr	L-threonine
HPG	L-P-hydroxy phenyl glycine	Trp	L-tryptophan
Hpglyo	4-hydroxy phenyl glyoxylate	Tyr	L-tyrosine

In addition to the CDA, *S. coelicolor* produces three other known antibiotics, actinorhodin, methylonomycin and undecylprodigiosin as well as a novel polyketide, mutactin. *S. coelicolor* has been used as a model microorganism for detailed and extensive genetic and physiological studies of streptomycetes (Hopwood, 1999). Optimised metabolic flux distributions were calculated for actinorhodin production in *S. coelicolor* for various nutrient limitations, and the effects of the type of nitrogen source on growth and actinorhodin production and metabolite excretion were investigated by Naeimpoor and Mavituna (2000, 2001). There is however, no publication yet on the quantified, experimental production of CDA.

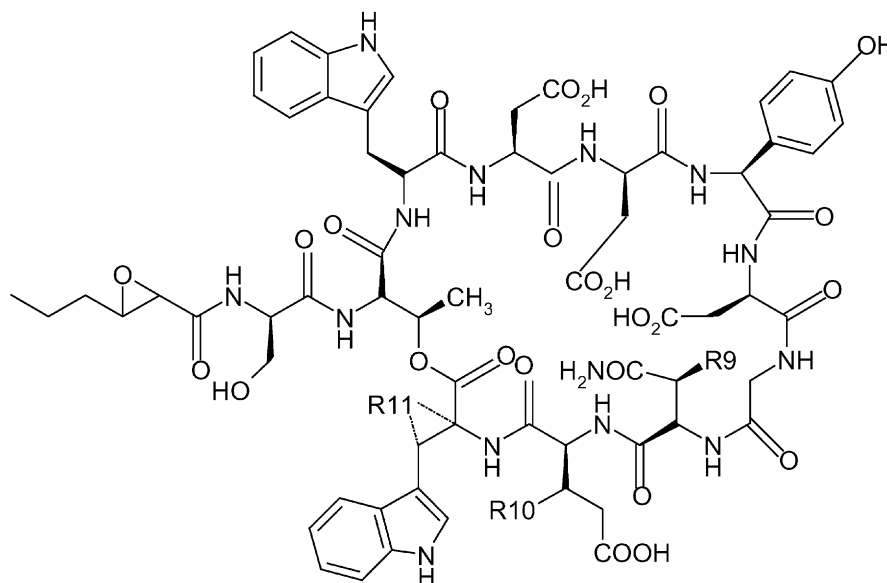
Peptide synthetases and the corresponding biosynthetic genes have been isolated from a variety of fungi

and bacteria including actinomycetes. There is an exciting scope for re-programming the peptide synthetases by the genetic mixing of the peptide synthetase modules to produce novel compounds (Hopwood et al., 1985; Madduri et al., 1998). There is therefore, considerable interest in the potential use of genetically engineered polyketide synthetases (PKSs) and peptide synthetases (PSs) for producing rationally designed polyketides and polypeptides as well as for combinatorial biosynthesis of libraries of novel unnatural molecules (McDaniel et al., 1994; Stachelhaus et al., 1996; Khosla, 1997; Hopwood, 1997; Cane et al., 1998; Staunton and Wilkinson, 2001; Walsh, 2002). Furthermore, mutant strains can be generated using genetic deletions to prevent the synthesis of a specific precursor so that altered precursors can be fed to these mutants which

Metabolic flux balancing can be used very effectively for such mutasynthesis and precursor-directed biosynthesis in order to predict the effects of genetic manipulations in silico and indicate alternative genetic engineering targets before costly and time consuming experimentation. It is therefore, timely to investigate the metabolic fluxes in *S. coelicolor* for CDA production in order to identify some targets for genetic engineering as well as some strategies for medium formulation and

2. Materials and methods for metabolic flux balancing in *S. coelicolor*

Only a few precursor structures are used in the formation secondary metabolites: coenzyme A derivatives of lower fatty acids, mevalonate (also derived from acetyl-CoA), amino acids, shikimate, sugars and nucleosides. These precursors are also needed in the primary metabolism to form the cellular building blocks. The CDA production therefore, starts from the primary metabolites which are necessary for growth. However,



CDAx	R ₉	R ₁₀	R ₁₁
CDA1b	OPO ₃ H ₂	H	H,H
CDA2a	OPO ₃ H ₂	CH ₃	π-bond
CDA2b	OPO ₃ H ₂	CH ₃	H,H
CDA3a	OH	H	π-bond
CDA3b	OH	H	H,H
CDA4a	OH	CH ₃	π-bond
CDA4b	OH	CH ₃	H,H

Fig. 1. Structure of the calcium dependent antibiotic of *S. coelicolor*.

the CDA is not necessary for growth. Like the other two antibiotics of *S. coelicolor*, actinorhodin and undecylprodigiosin, the CDA is also derived from Acetyl-CoA and Malonyl-CoA. As well as D-4-hydroxyphenylglycine (HPG), which is produced in the pentose phosphate pathway, CDA is a very complex nonribosomal lipopeptide made up of a cyclic lactone undecapeptide with an *N*-terminal 2,3-epoxyhexanoyl fatty acid side chain, several D-configured and unusual amino acids, including D-4-hydroxyphenylglycine, D-3-phosphohydroxyasparagine, and L-3-methylglutamic acid (Kempster et al., 1997; Hojati et al., 2002). As shown in Fig. 1, CDA has variable amino acid residues at four different positions. The amino acids required for CDA biosynthesis are tyrosine, aspartate, asparagine, tryptophan, threonine, glycine, serine, glutamate and oxoglutarate.

We summarised the reactions of the CDA biosynthesis in Table 1 using the work of Hojati et al. (2002) and annotations from the genome scale analysis available at KEGG (www.genome.ad.jp) and Sanger Centre websites (www.sanger.ac.uk).

2.2. Metabolic model of *S. coelicolor*

Secondary metabolites are often produced from primary metabolites, which are themselves produced from 20 key metabolite precursors (Stephanopoulos et al., 1998). It is therefore, necessary to include all the major pathways of primary metabolism in any metabolic modelling of secondary metabolite production but especially in this case since the CDA production consumes a significant amount of amino acids. The biochemical reaction network used in this work to model *S. coelicolor* metabolism was very similar to that described in Naeimpoor and Mavituna (2000, 2001) and

Takac et al. (1998). It was however, expanded to contain over 400 biochemical reactions of the major metabolic pathways such as glycolysis, pentose phosphate (PP), tricarboxylic acid (TCA), glyoxylate, as well as the anaplerotic reactions, sulphate assimilation, electron transport, folic acid and thioredoxin reactions, the biosynthesis of aromatic, aspartate, glutamate, pyruvate, serine family amino acids and histidine, the biosynthesis of pyrimidine and purine nucleotides, the biosynthesis of macromolecular components of biomass such as RNA, DNA, protein, phospholipids, carbohydrate and CDA production. The biosynthetic pathways for CDA were derived from the literature (Hojati et al., 2002). The excretion of pyruvate, acetate, formate, glycerol, and CDA is also allowed in our computational programme.

The amount of protein, RNA and DNA in the dry biomass of *S. coelicolor* was taken from Shahab et al. (1996). The phospholipid content of the biomass was assumed to be the same as *E. coli* (Ingraham et al., 1983) and the rest of the biomass was assumed to be made up of carbohydrate. The amount of precursors required to produce one gram of protein, RNA, DNA and phospholipids as well as the polymerisation energies required for the biosynthesis of these macromolecules were assumed to be the same as in *E. coli* (Ingraham et al., 1983). The cell composition was assumed constant. P/O ratio was assumed to be 1.9 in the NADH oxidation reactions and two thirds of this amount for the FADH₂ oxidation reactions.

The mathematical model was based on metabolic flux balancing and consisted of a set of linear algebraic equations obtained by applying pseudo-steady-state mass balance for all metabolites and neglecting the changes in pool metabolites. The underdetermined set of

Table 1
Summary of the metabolic reactions for the CDA biosynthesis

PEP + O ₂	→	Hmana + CO ₂
2*Hmana + O ₂	→	2*Hpglyo
Hpglyo + Tyrosine	↔	HPG + PEP
AcCoA + 2*MaCoA + 4*NADPH	↔	Hexaa + 2*CO ₂ + 4*NADP ⁺ + 3*CoA
Hexaa + CoA + ATP	↔	CoAthio + AMP + PP _i
CoAthio + FAD	→	ThexCoA + FADH ₂
FADH ₂ + O ₂	→	FAD
ThexCoA + FADH-OOH	→	TehCoA + FADH-OH
FADH ₂ + O ₂	→	FADH-OOH
FADH-OH	→	FAD
FAD + 2*NADH	→	FADH ₂ + 2*NAD ⁺
OG + O ₂ + AdoMet	→	AdoHcy + MOG
MOG + PMP	→	MeGlu + PLPC
Glu + PLPC	→	OG + PMP
ThexCoA + HPG + 3*Asp + 2*Trp + Thr + Gly + Ser + MeGlu + Asn + 11*ATP	→	CDAx + CoA + 11*AMP + 11*PP _i
CDAx + O ₂ + OG	→	CDA4b + Suc
CDA4b + ATP	→	CDA4a + ADP
CDA4a + FAD	→	CDA + FADH ₂

linear equations could only be solved by optimising a defined objective function (Stephanopoulos et al., 1998). In this work the objective function was defined as either the specific growth rate or the specific CDA production rate and the maximisation of the objective function was the direction of optimisation. The solution then gave not only the maximum value of the objective function but also the values of the unknown metabolic fluxes, including the specific substrate uptake and product formation rates, within the network in $\text{mmol (g dry weight)}^{-1} \text{h}^{-1}$. It should be noted that the solution presents a theoretical case in which all the calculated fluxes are the optimised values needed to achieve the objective of optimisation. The experimental values for specific growth and glucose uptake rates from a batch culture of *S. coelicolor* (Ozergin, 1991) were used as constraints in the solution of the model for the specific

CDA production rate maximisation. For the maximisation of the specific growth rate, only the experimental value of the specific glucose uptake rate was used as the constraint in the solution. The underdetermined set of linear equations resulting from metabolic flux balancing was solved by linear optimisation using GAMS software (Brooke et al., 1992) to determine the optimised metabolic flux distributions for various cases (Takac et al., 1998).

3. Results and discussion

3.1. Optimised metabolic flux distributions

A typical batch culture of *S. coelicolor* is shown in Fig. 2 (Ozergin, 1991). The 20 L bioreactor containing

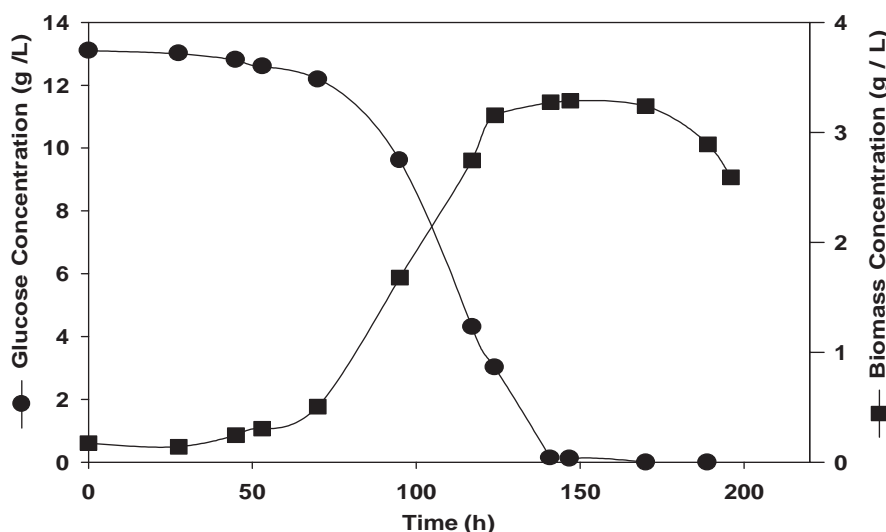


Fig. 2. A typical batch culture of *S. coelicolor* in a 20 L bioreactor using defined medium with 13 g/L glucose and 15% v/v vegetative inoculum.

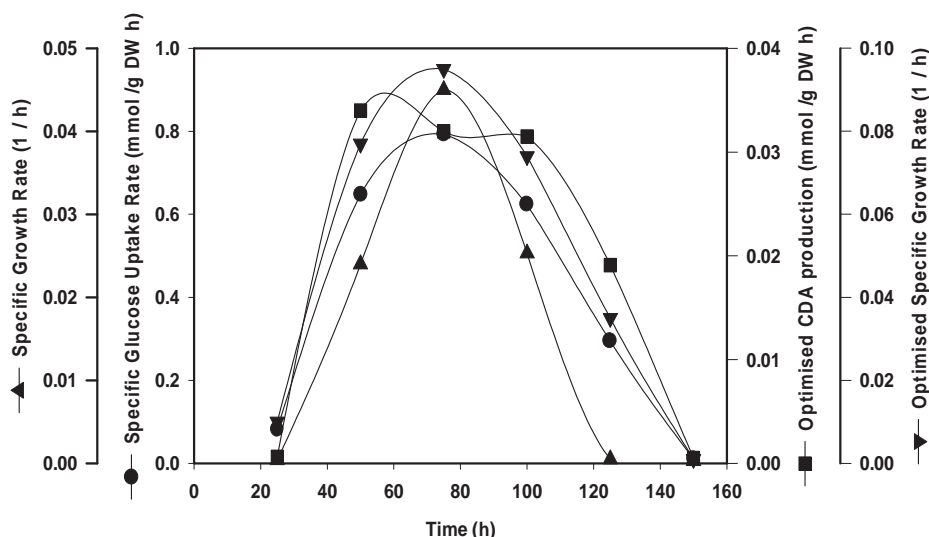


Fig. 3. Experimental and optimised (maximised) specific rates.

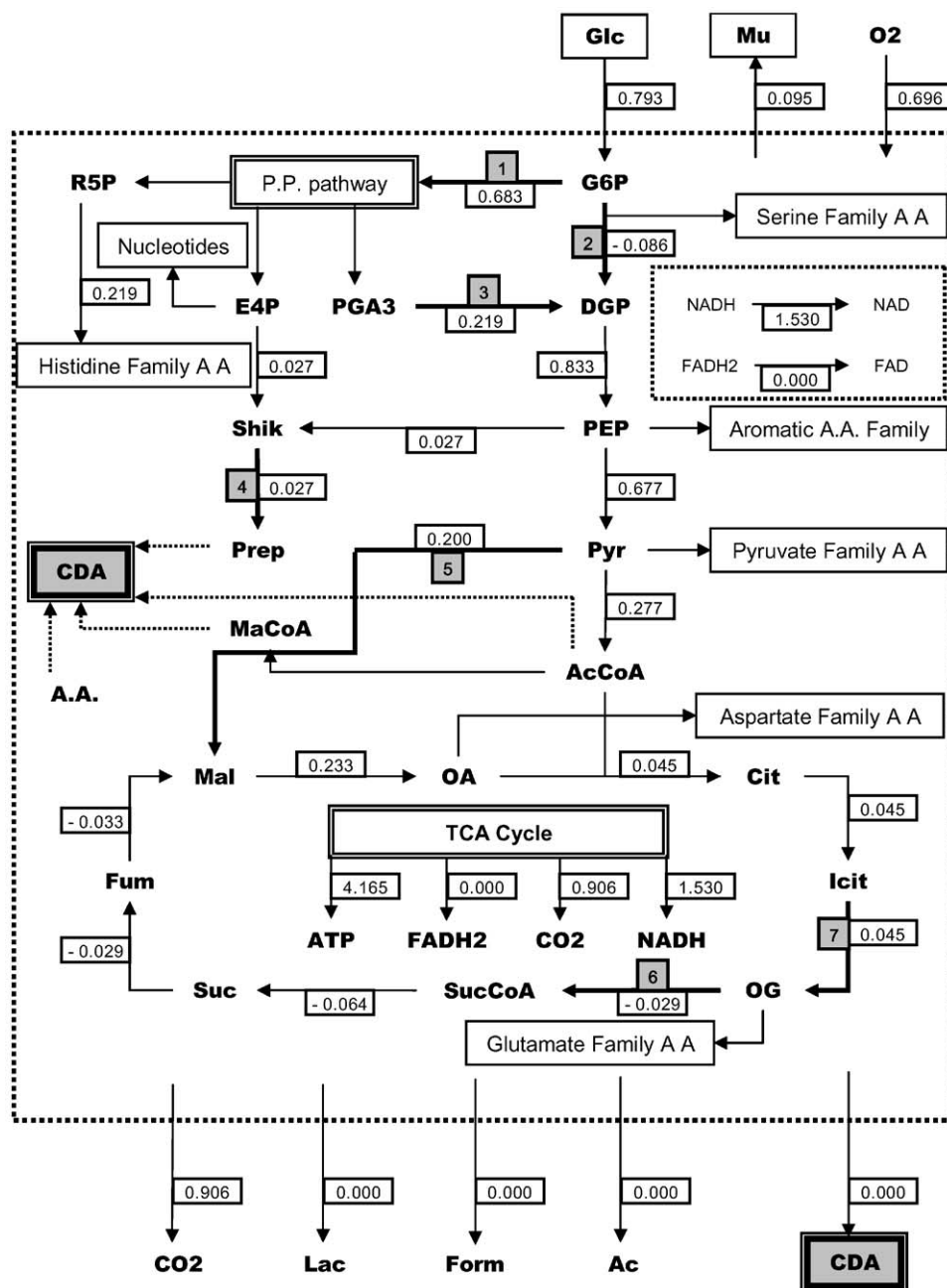


Fig. 4. Metabolic fluxes during the maximisation of specific growth rate of *S. coelicolor* at the 75th h of the batch.

12 L of defined medium was inoculated with 15% v/v vegetative inoculum. The details of medium composition and experimental procedures are given in Ozerin-Ulgen and Mavituna (1993). Carbon and energy source was glucose and the nitrogen source was nitrate. We are developing a quantitative method for CDA analysis based on LC-MS currently and therefore do not have experimental data on the CDA production yet. In fact, there is no quantitative experimental data available in the literature on the CDA production.

We calculated the specific growth and glucose uptake rates from this set of experimental data at every 25 h

interval for the duration of the batch culture. Using the experimental specific glucose uptake rate as a constraint and the maximisation of the specific growth rate as the objective function in the computational model, we calculated the optimised (maximised) specific growth rates for different phases of the batch. We then used both the experimental specific growth and glucose uptake rates as the constraints and the maximisation of the specific CDA production rate as the objective function in the computational model, to calculate the optimised (maximised) specific CDA production rates. These experimental and maximised

specific rates are compared in Fig. 3. These results indicate that the experimental specific growth rates are about half of the optimum values. This is expected since the procedure used is not a model fitting exercise and the experiment was not conducted under optimised conditions.

In fact, this is an indication that *S. coelicolor* culture is not utilising its full theoretical biological capacity for growth. The computed CDA specific production rates indicate that despite being a secondary metabolite, CDA production at least theoretically coincides with growth. The computed specific CDA production rate reaches a

peak around the 50th h of the batch which is earlier than the peaks in the experimental and computed specific growth rates, as well as the experimental specific glucose uptake rate (Fig. 3).

Optimisation of the objective function for the solution of the metabolic flux balances also gives the individual fluxes of over 400 metabolic reactions. Since it is not possible to represent all these visually, only a summary of the most significant fluxes are presented in Figs. 4 and 5. In these figures, the values of the fluxes are given in rectangles attached to the arrows. Their units are in $\text{mmol (g dry weight)}^{-1} \text{h}^{-1}$. A negative sign indicates

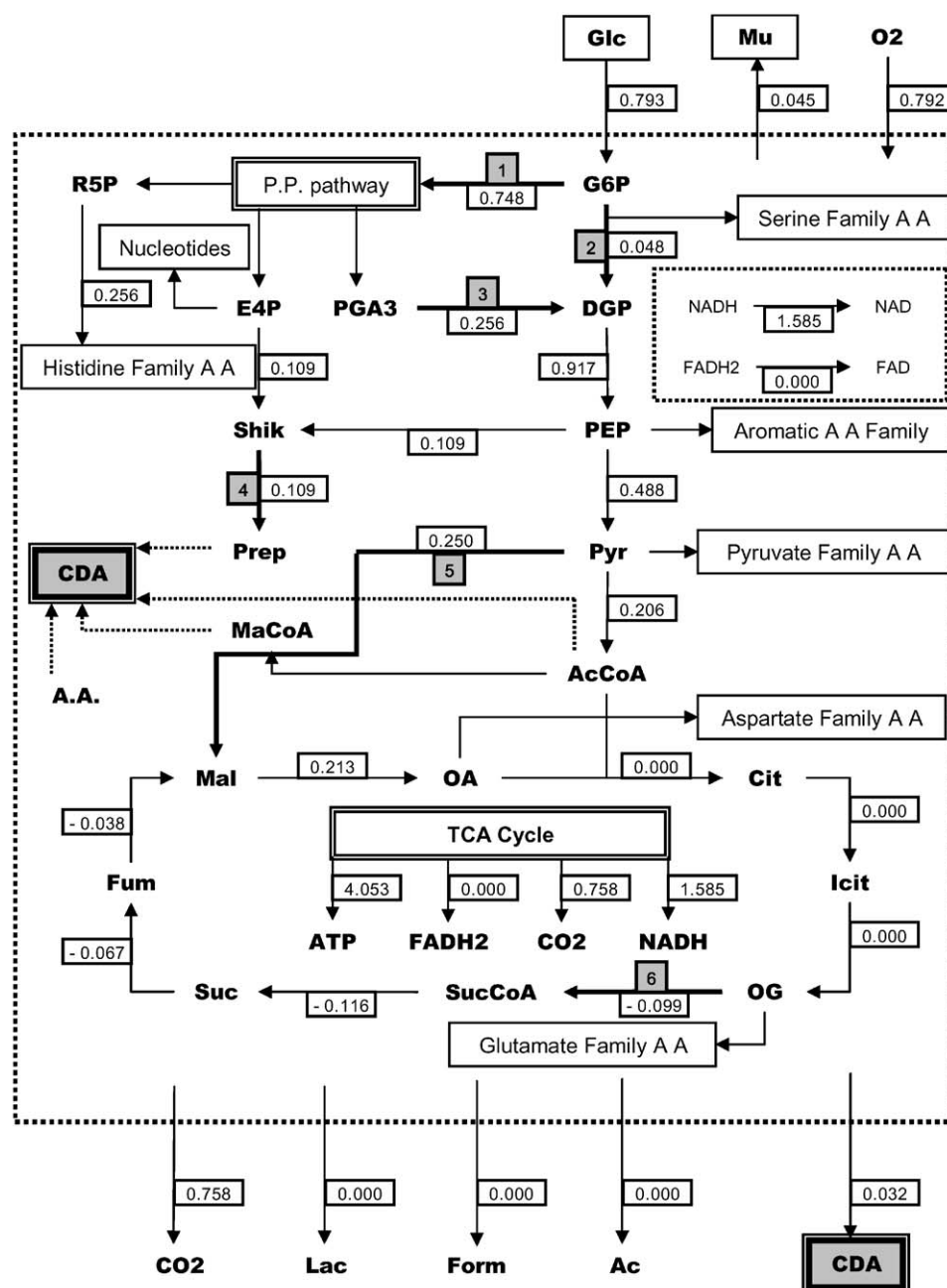


Fig. 5. Metabolic fluxes during the maximisation of specific CDA production rate of *S. coelicolor* at the 75th h of the batch.

that the reaction proceeds in the opposite direction of the arrow.

Fig. 4 gives the values of some of the metabolic fluxes for the maximisation of growth rate using the experimental specific glucose uptake rate as a constraint at the 75th h of the batch. Similarly, Fig. 5 is for the maximisation of the specific production rate of the CDA using the experimental values of the specific growth and glucose uptake rates as constraints. When this analysis was performed for the duration of the batch culture, from 25 to 150 h, the most significant changes were observed only in a small number of metabolic fluxes while the rest of the fluxes either showed insignificant changes or did not change at all. These significant metabolic fluxes are listed in Table 2 and are indicated on the flux maps of Figs. 4 and 5 with bold arrows. The numbers in boxes next to the bold arrows in Figs. 4 and 5 correspond to the pathway numbers used in Table 2. The values of these fluxes during different phases of the batch culture are shown in Figs. 6 and 7.

According to Figs. 4 and 5, most of the glucose taken up is directed to the pentose phosphate pathway during the maximisation of specific growth and CDA production rates. This was also found by Obanye et al. (1996) who studied the Embden–Meyerhof–Parnas (EMP) and pentose phosphate (PP) pathway fluxes using radio-respirometry in *S. coelicolor*. They reported that during the exponential growth phase the carbon flux passing through the pentose phosphate pathway was less than that through the EMP pathway. It increased and even exceeded that through the EMP pathway when growth declined and methylenomycin was being produced. Growth and especially CDA production require reducing power in the form of NADPH. Most of this is supplied from the PP pathway and this is the reason why fluxes associated with the PP pathway are the most changeable ones in Figs. 4 and 5 during batch growth and CDA production.

During growth maximisation, the TCA cycle was completed. During the maximisation of CDA produc-

Table 2

Fluxes that show the most pronounced changes in the calculated flux distribution maps for growth and CDA optimisation over the duration (25–150 h) of *S. coelicolor* batch culture of Fig. 2. These are indicated by their relevant pathway numbers on the flux maps of Figs. 4 and 5. The values of these fluxes are given in Figs. 6 and 7

Pathway number	Metabolic reaction
1	$\text{G6P} + \text{NADP} \rightarrow \text{NADPH} + \text{PGnL6}$
2	$\text{G6P} \rightarrow \text{F6P}$
3	$\text{PGA3} + \text{S7P} \rightarrow \text{F6P} + \text{E4P}$
4	$\text{Shik} + \text{ATP} \rightarrow \text{ADP} + \text{PShik3}$
5	$\text{Pyr} + \text{CO}_2 + \text{NADPH} \rightarrow \text{NADP} + \text{Mal}$
6	$\text{OG} + \text{CoA} + \text{NAD} \rightarrow \text{NADH} + \text{CO}_2 + \text{SucCoA}$
7	$\text{ICit} + \text{NADP} \rightarrow \text{NADPH} + \text{CO}_2 + \text{OG}$

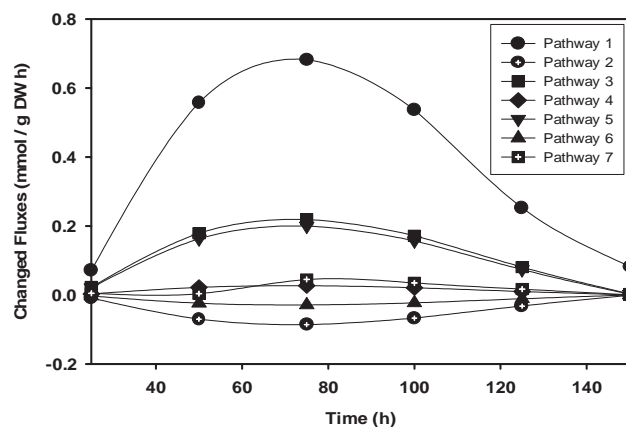


Fig. 6. Values of the fluxes with the most significant changes during the batch culture for the specific growth rate maximisation. Pathway reactions are given in Table 2.

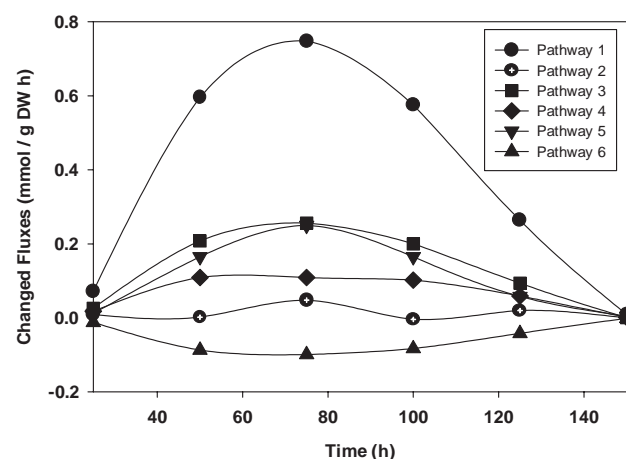


Fig. 7. Values of the fluxes with the most significant changes during the batch culture for the maximisation of specific CDA production rate. Pathway reactions are given in Table 2.

tion however, citrate and isocitrate fluxes were zero and the fluxes were reversed from malate towards oxoglutarate. The importance of the oxoglutarate associated fluxes can be explained by the role of these in nitrogen assimilation. The inorganic nitrogen can only be incorporated into the biomass via the biosynthesis of glutamate and glutamine. When the nitrogen source is nitrate or urea, the inorganic nitrogen must first be converted to ammonia which could then diffuse through the cytoplasmic membranes to serve as an amino group in glutamate and glutamine (Shapiro, 1989). Glutamate then donates the amino group to most of the amino acids while glutamine supplies the amino group to histidine, tryptophan and asparagine. Glutamine is also the amino donor for compounds such as pyrimidines and purines. Oxoglutarate from the TCA cycle is linked to both glutamate and glutamine fluxes.

This is why oxoglutarate is important for maximisation of growth and CDA production. Pyruvate to malate flux is another significant one since it feeds the TCA cycle with carbohydrate while acetyl-CoA is used for the CDA synthesis. Although pyruvate to acetyl-CoA flux is also important, the pyruvate to malate flux changes more. The reason as to why the shikimate to prephenate flux shows significant changes is obvious; prephenate is the most important building block of the CDA.

3.2. Sensitivity analysis

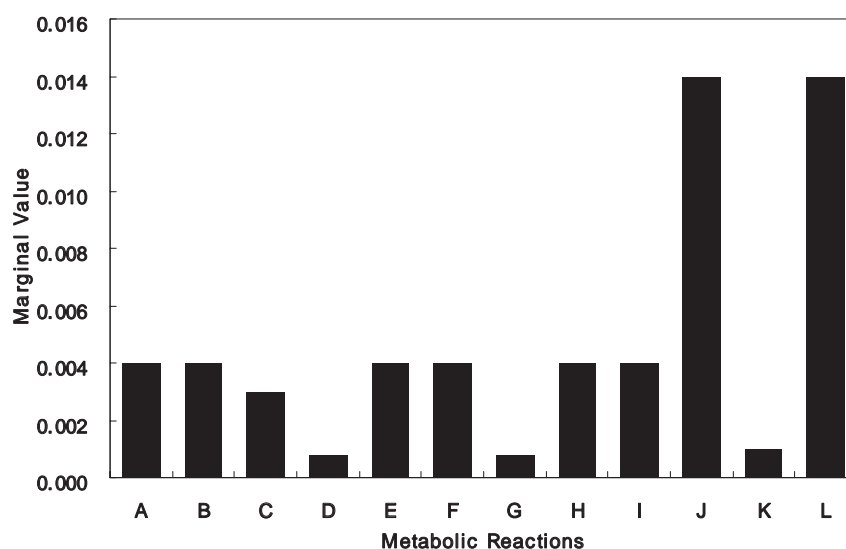
One of the advantages of GAMS software used for the optimisation of the metabolic flux model is the calculation of marginal values of the majority of intermediate metabolites and the metabolic pathways. The marginal values can be viewed as the sensitivity of the objective function for the changes in a variable.

These sensitivities are shown in terms of marginal values in Figs. 8 and 9 for the maximisation of the specific growth and CDA production rates, respectively, for the 50th h of the batch. For example, the marginal value of nitrate assimilation pathway S of Fig. 9 is 0.026. This means that a change of 1 unit in the nitrate assimilation flux can affect the value of the specific CDA production rate by 0.026 units.

According to Fig. 8, aspartate family of amino acids and the CDA biosynthesis seem to play significant roles in the maximisation of the specific growth rate. Nitrate assimilation pathway is the most important flux in the maximisation of the CDA production in silico.

3.3. Targets for genetic engineering

We demonstrated in Fig. 5 that fluxes associated with prephenate and oxoglutarate are significant for CDA production. Furthermore, the sensitivity analysis shown



Legends for metabolic reactions

A	$\text{F6P} \rightarrow \text{G6P}$
B	$\text{Gro} + \text{ATP} \rightarrow \text{ADP} + \text{GL3P}$
C	$\text{OA} + \text{ATP} \rightarrow \text{ADP} + \text{CO}_2 + \text{PEP}$
D	$\text{PEP} + \text{CO}_2 \rightarrow \text{Pi} + \text{OA}$
E	$\text{ICit} \rightarrow \text{Suc} + \text{Glx}$
F	$\text{Pyr} + \text{CoA} + \text{NADH} \rightarrow \text{NAD} + \text{Form} + \text{AcCoA}$
G	$\text{Gln} + \text{OG} + \text{NADH} \rightarrow \text{NAD} + 2 \text{Glu}$
H	$\text{Form10THF} \rightarrow \text{Form} + \text{THF}$
I	$\text{Gln} + \text{CO}_2 + \text{ATP} \rightarrow \text{ADP} + \text{Glu} + \text{CbmP}$
J	$\text{SucHse} + \text{Cys} \rightarrow \text{Suc} + \text{Cyst}$
K	$\text{Gly} + \text{THF} + \text{NAD} \rightarrow \text{NADH} + \text{MeTHF} + \text{CO}_2 + \text{NH}_3$
L	$\text{FADH}_2 + \text{O}_2 \rightarrow \text{FAD}$

Fig. 8. Sensitivity of the specific growth rate for changes in various fluxes in terms of the marginal values at the 50th h of the batch.

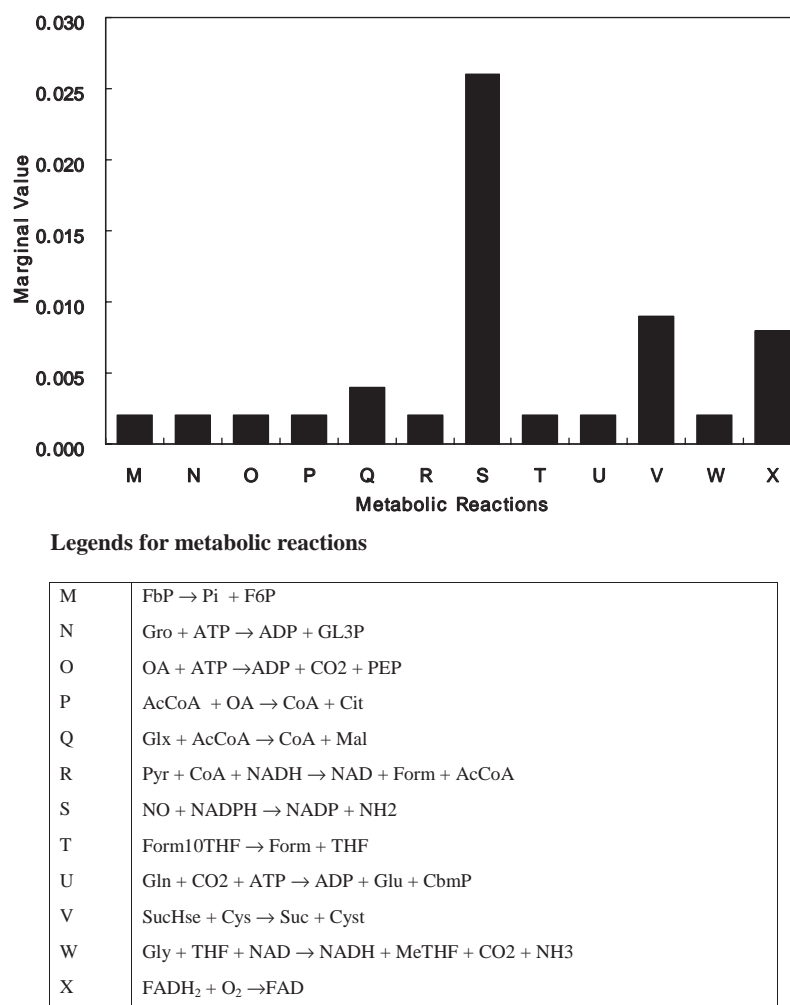


Fig. 9. Sensitivity of the specific CDA production rate for changes in various fluxes in terms of the marginal values at the 50th h of the batch.

in Fig. 9 indicated that the fluxes associated with nitrogen assimilation, succinate and flavine adenine dinucleotide production also play important roles in CDA production. When the metabolic pathways involving these metabolites and fluxes are studied in conjunction with the known enzymes of these reactions from databases such as www.kegg.com and www.sanger.ac.uk, it becomes obvious that some genetic manipulation may lead to the increased CDA production. Genetic deletions work by eliminating wasteful use of an important precursor or a metabolite in side-reactions. Compared to the genetic amplifications, deletions can be studied more easily both in silico and in vitro because deletion means a zero flux whereas amplification can have a wide range of values. One should however, be careful not to create lethal deletions. It is therefore, less risky if these deletions are not around the important pathways of the primary metabolism. Furthermore, the product of the deleted reaction should be produced by another route so that the metabolism

does not suffer. We therefore, chose the anthranilate and L-glutamate biosynthesis as the targets for in silico genetic engineering. Fig. 10 indicates which deletions in anthranilate pathway should in theory increase prephenate flux. Similarly, Fig. 11 indicates how deletions in L-glutamate biosynthesis should in theory increase oxoglutarate. Table 3 gives the genes and gene products (enzymes) associated with these pathway deletions.

These deletions were carried out in our metabolic model and the results of these in silico genetic deletions are given in Fig. 12. Here, the control is the maximised specific CDA production rate with the normal metabolism at the conditions of the 50th h of the batch culture. Deletions in oxoglutarate pathway and anthranilate pathway results in higher CDA production rates. According to Fig. 12, oxoglutarate associated deletions can increase CDA production as much as three times. This demonstrates the power of metabolic flux balancing tool for the determination of targets for feasible genetic engineering for the desired metabolic effects.

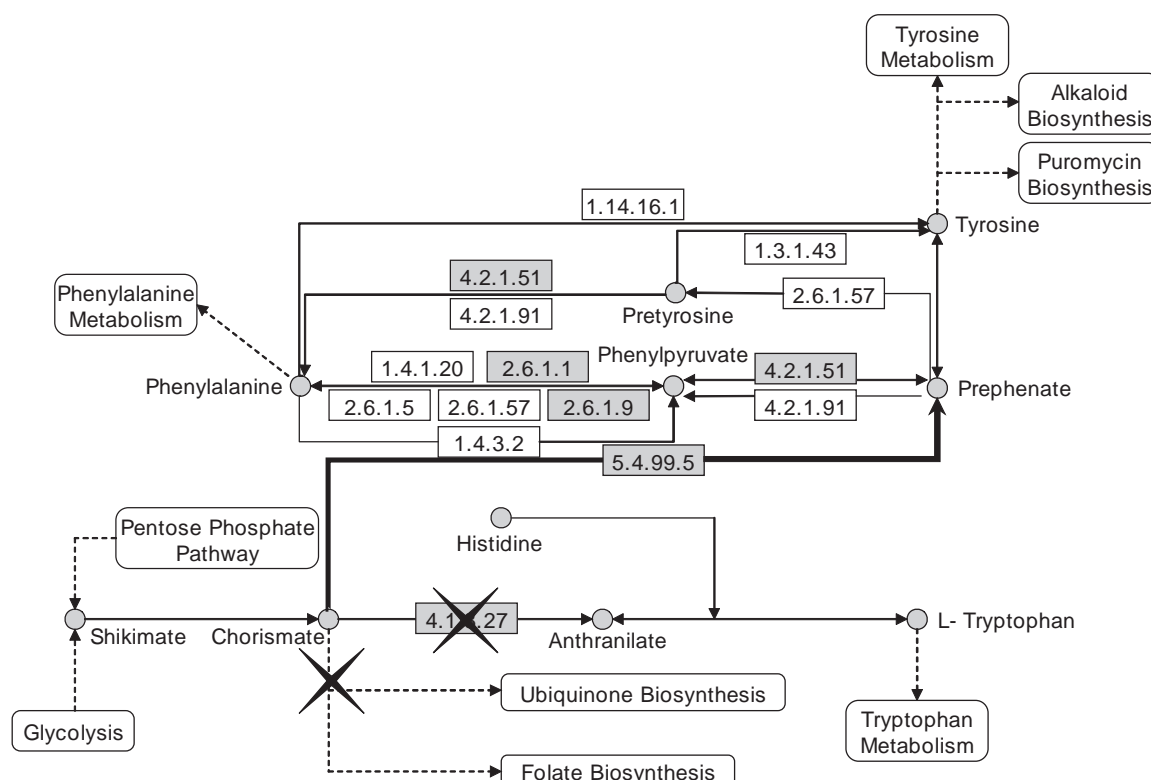


Fig. 10. Deletions indicated with crosses in the anthranilate biosynthesis pathway (from www.kegg.com).

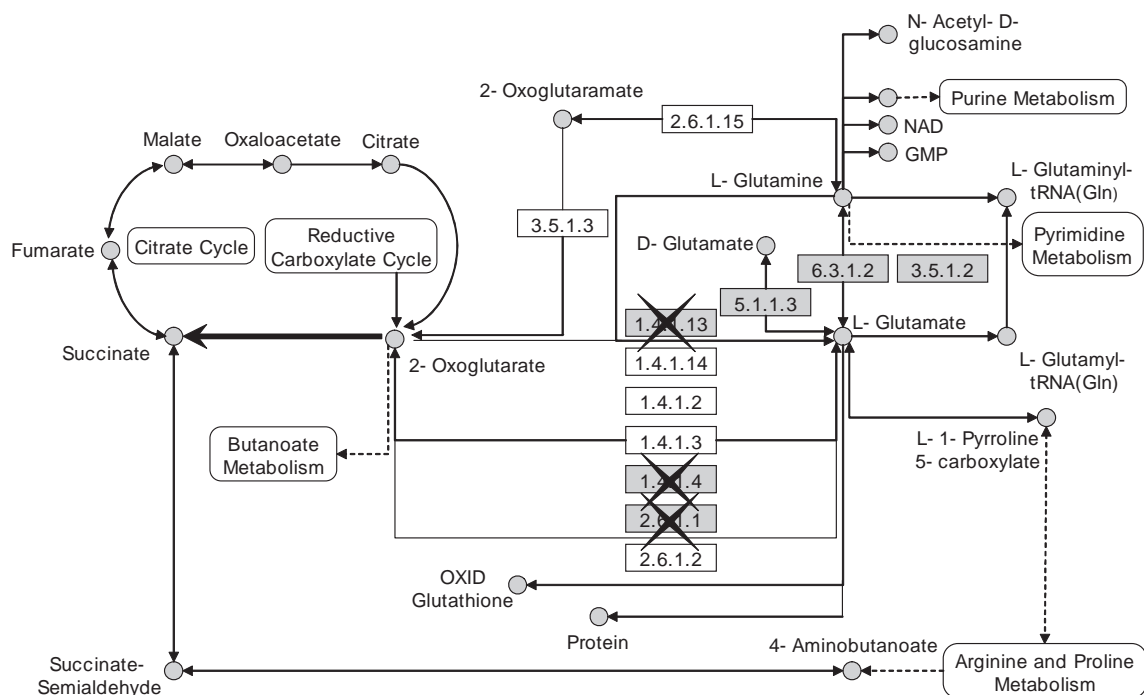


Fig. 11. Deletions indicated with crosses in the L-glutamate biosynthesis pathway (from www.kegg.com).

4. Conclusions

From a biosynthetic point of view, non-ribosomally synthesised peptides are one of the most interesting

classes of natural products displaying a wide range of biological activity (Kleinkauf and von Dohren, 1996; Stein and Vater, 1996; Chong et al., 1998). Production of novel natural and unnatural products

Table 3

The target pathways for genetic deletions, and the associated enzymes and genes in *S. coelicolor* to increase CDA production (www.kegg.com and www.sanger.ac.uk)

Pathway	Gene target for deletion	Enzyme affected
Anthranilate synthesis	SC4G6.12c	EC 4.1.3.27
L-glutamate synthesis	SC3C9.12	EC 1.4.1.13
	SCD31.08	EC 1.4.1.4
	SCD82.16c	EC 2.6.1.1

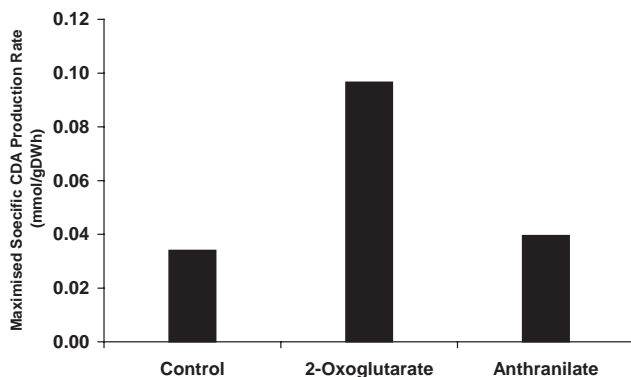


Fig. 12. The effect of genetic deletions in the oxoglutarate and anthranilate pathways on the maximised specific CDA production rates compared to the normal metabolism of the control.

via precursor-directed mutasynthesis in *Streptomyces* and other microorganisms using natural and recombinant polyketide synthetases and peptide synthetases promises new drugs in our fight against life-threatening infections and diseases. Metabolic flux balancing can be used as an effective tool for the study and elucidation of the metabolic pathways in such organisms, for media formulation and determination of bioreactor operational strategies, and targeting genetic manipulations. In this research, we gave an example of the application of metabolic flux balancing for the optimisation of growth and CDA production rates in *S. coelicolor*. The results indicated that CDA production was concomitant with the growth of *S. coelicolor*, which was also found experimentally with actinorhodin production in the same microorganism in a previous study (Ozergin-Ulgen and Mavituna, 1993). The metabolic flux distributions and sensitivity analyses during various phases of the batch culture indicated that specific CDA production rate was affected by nitrogen assimilation, pentose phosphate pathway, shikimate biosynthesis, and oxoglutarate fluxes. Consequently, this was tested by in silico genetic deletions which resulted in increased specific CDA production rates. Of course, such in silico experiments should be verified by in vitro genetic engineering investigations. Nevertheless, in silico studies like this work may save valuable time and money by indicating the strategic genetic targets.

References

- Bentley, S.D., Chater, K.F., Cerdeno-Tarraga, A.M., Challis, G.L., Thomson, N.R., James, K.D., Harris, D.E., Quail, M.A., Kieser, H., Harper, D., Bateman, A., Brown, S., Chandra, G., Chen, C.W., Collins, M., Cronin, A., Fraser, A., Goble, A., Hidalgo, J., Hornsby, T., Howarth, S., Huang, C.H., Kieser, T., Larke, L., Murphy, L., Oliver, K., O'Neil, S., Rabinowitsch, E., Rajandream, M.A., Rutherford, K., Rutter, S., Seeger, K., Saunders, D., Sharp, S., Squares, R., Squares, S., Taylor, K., Warren, T., Wietzorrek, A., Woodward, J., Barrell, B.G., Parkhill, J., Hopwood, D.A., 2002. Complete genome sequence of the model actinomycete *Streptomyces coelicolor* A3(2). *Nature* 9.417 (6885), 141–147.
- Brooke, A., Kendrick, D., Meeraus, A., 1992. GAMS-A User Guide. Scientific Press, Redwood City.
- Cane, D.E., Walsh, C.T., Khosla, C., 1998. Harnessing the biosynthetic code: combinations, permutations, and mutations. *Science* 282, 63–68.
- Chong, P.P., Podmore, S.M., Kieser, H.M., Redenbach, M., Turgay, K., Marahiel, M., Hopwood, D.A., Smith, C.P., 1998. Physical identification of a chromosomal locus encoding biosynthetic genes for the lipopeptide calcium-dependent antibiotic (CDA) of *Streptomyces coelicolor* A3(2). *Microbiology* (Reading, UK) 144 (1), 193–199.
- Hojati, Z., Milne, C., Harvey, B., Gordon, L., Borg, M., Flett, F., Wilkinson, B., Sidebottom, P.J., Rudd, B.A.M., Hayes, M.A., Smith, C.P., Micklefield, J., 2002. Structure, biosynthetic origin, and engineered biosynthesis of calcium-dependent antibiotics from *Streptomyces coelicolor*. *Chem. Biol.* 9 (11), 1175–1187.
- Hopwood, D.A., 1997. Genetic contributions to understanding polyketide synthases. *Chem. Rev.* 97, 2465–2497.
- Hopwood, D.A., 1999. Forty years of genetics with *Streptomyces*: from in vivo through in vitro to in silico. *Microbiology* 145, 2183–2202.
- Hopwood, D.A., Malpartida, F., Kieser, H.M., Ikeda, H., Duncan, J., Fujii, I., Rudd, B.A.M., Floss, H.G., Omura, S., 1985. Production of “hybrid” antibiotics by genetic engineering. *Nature* 314, 642–644.
- Hopwood, D.A., Wright, H.M., 1983. CDA is a new chromosomally determined antibiotic from *Streptomyces coelicolor* A3(2). *J. Gen. Microbiol.* 129 (12), 3575–3579.
- Ingraham, J.L., Maaloe, O., Neidhardt, F.C., 1983. Growth of the Bacterial Cell. Sinauer Associates, Sunderland.
- Kempler, C., Kaiser, D., Haag, S., Nicholson, G., Gnau, V., Walk, T., Gierling, K.H., Decker, H., Zaehner, H., Jung, G., Metzger, J.W., 1997. CDA: calcium-dependent peptide antibiotics from *Streptomyces coelicolor* A3(2) containing unusual residues. *Angew. Chem. Int. Ed. Eng.* 36 (5), 498–501.
- Khosla, C., 1997. Harnessing the biosynthetic potential of modular polyketide synthases. *Chem. Rev.* 97, 2577–2590.
- Madduri, K., Kennedy, J., Rivola, G., Inventi-Solari, A., Filippini, S., Zanusso, G., Colombo, A.L., Gewain, K.M., Occi, J.L., MacNeil, D.J., et al. 1998. Production of the antitumor drug epirubicin (4'-epidoxorubicin) and its precursor by a genetically engineered strain of *Streptomyces peucetius*. *Nat. Biotechnol.* 16, 69–74.
- McDaniel, R., Ebert-Khosla, S., Hopwood, D.A., Khosla, C., 1994. Engineered biosynthesis of novel polyketides: influence of a downstream enzyme on the catalytic specificity of a minimal aromatic polyketide synthase. *Proc. Natl. Acad. Sci. Biochem.* 91, 11542–11546.
- Naeimpoor, F., Mavituna, F., 2000. Metabolic flux analysis in *Streptomyces coelicolor* under various nutrient limitations. *Metab. Eng.* 2 (2), 140–148.
- Naeimpoor, F., Mavituna, F., 2001. Metabolic flux analysis in *Streptomyces coelicolor*: effect of nitrogen source. In: Van

- Broekhoven, A., Shapiro, F., Anne, J. (Eds.), Novel Frontiers in the Production of Compounds for Biomedical Use, Vol. 1. Kluwer Academic Publishers, Dordrecht, The Netherlands, pp. 131–145.
- Obanye, A.I.C., Hobbs, G., Gardner, D.C.J., Oliver, S.G., 1996. Correlation between carbon flux through the pentose phosphate pathway and production of the antibiotic methylenomycin in *Streptomyces coelicolor* A3(2). *Microbiology* 142, 133–137.
- Omura, S., Ikeda, H., Ishikawa, J., Hanamoto, A., Takahashi, C., Shinose, M., Takahashi, Y., Horikawa, H., Nakazawa, H., Osonoe, T., Kikuchi, H., Shiba, T., Sakaki, Y., Hattori, M., 2001. Genome sequence of an industrial microorganism *Streptomyces avermitilis*: deducing the ability of producing secondary metabolites. *Proc. Natl. Acad. Sci. USA* 98, 12215–12220.
- Ozergin, K.S., 1991. Study of antibiotic synthesis by free and immobilised *Streptomyces coelicolor* A3(2). Ph.D. Thesis, Victory University of Manchester, Manchester, UK.
- Ozergin-Ulgen, K., Mavituna, F., 1993. Actinorhodin production by *Streptomyces coelicolor* A3(2): kinetic parameters related to growth, substrate uptake and production. *Appl. Microbiol. Biotechnol.* 40, 457–462.
- Raja, A., LaBorte, J., Lebbos, J., Kirkpatrick, P., 2003. Fresh from the pipeline: Daptomycin. *Nature Rev., Drug Discovery*, 2, 943–944.
- Ryding, N.J., Anderson, T.B., Champness, W.C., 2002. Regulation of the *Streptomyces coelicolor* calcium-dependent antibiotic by *absA*, encoding a cluster-linked two-component system. *J. Bacteriol.* 184, 794–805.
- Shahab, N., Flett, F., Oliver, S.G., Butler, P.R., 1996. Growth rate control of protein and nucleic acid content in *Streptomyces coelicolor* A3(2) and *Escherichia coli* B/r. *Microbiology* 142, 1927–1935.
- Shapiro, S., 1989. Nitrogen assimilation in actinomycetes and the influence of nitrogen nutrition on actinomycete secondary metabolism. In: Shapiro, S. (Ed.), Regulation of Secondary Metabolism in Actinomycetes. CRC Press, Boca Raton, FL, pp. 135–213.
- Stachelhaus, T., Schneider, A., Marahiel, M.A., 1996. Engineered biosynthesis of peptide antibiotics. *Biochem. Pharmacol.* 52, 177–186.
- Staunton, J., Wilkinson, B., 2001. Combinatorial biosynthesis of polyketides and nonribosomal peptides. *Curr. Opin. Chem. Biol.* 5, 159–164.
- Stein, T., Vater, J., 1996. Amino acid activation and polymerisation at modular multienzymes in non-ribosomal peptide biosynthesis. *Amino Acids* 10, 201–227.
- Stephanopoulos, G.N., Aristidou, A.A., Nielsen, J., 1998. Metabolic Engineering: Principles and Methodologies. Academic Press, San Diego.
- Takac, S., Calik, G., Mavituna, F., Dervakos, G., 1998. Metabolic flux distribution for the optimised production of L-glutamate. *Enzyme Microbial Technol.* 23, 286–300.
- Walsh, C.T., 2002. Combinational biosynthesis of antibiotics: challenges and opportunities. *Chembiochem* 3, 124–124.
- Wohlleben, W., Pelzer, S., 2002. New compounds by combining “modern” genomics and “old-fashioned” mutasynthesis. *Chem. Biol.* 9 (11), 1163–1164.